Exosomes From Adipose-Derived Stem Cells Attenuate Adipose Inflammation and Obesity Through Polarizing M2 Macrophages and Beiging in White Adipose Tissue

Hui Zhao,[1] Qianwen Shang,[1] Zhenzhen Pan,[1] Yang Bai,[1] Zequn Li,[1] Huiying Zhang,[1] Qiu Zhang,[2] Chun Guo,[1] Lining Zhang,[1] and Qun Wang[1]

Diabetes 2018;67:235–247 | https://doi.org/10.2337/db17-0356

Adipose-derived stem cells (ADSCs) play critical roles in controlling obesity-associated inflammation and metabolic disorders. Exosomes from ADSCs exert protective effects in several diseases, but their roles in obesity and related pathological conditions remain unclear. In this study, we showed that treatment of obese mice with ADSC-derived exosomes facilitated their metabolic homeostasis, including improved insulin sensitivity (27.8% improvement), reduced obesity, and alleviated hepatic steatosis. ADSC-derived exosomes drove alternatively activated M2 macrophage polarization, inflammation reduction, and beiging in white adipose tissue (WAT) of diet-induced obese mice. Mechanistically, exosomes from ADSCs transferred into macrophages to induce anti-inflammatory M2 phenotypes through the transactivation of arginase-1 by exosome-carried active STAT3. Moreover, M2 macrophages induced by ADSC-derived exosomes not only expressed high levels of tyrosine hydroxylase responsible for catecholamine release, but also promoted ADSC proliferation and lactate production, thereby favoring WAT beiging and homeostasis in response to high-fat challenge. These findings delineate a novel exosome-mediated mechanism for ADSC–macrophage cross talk that facilitates immune and metabolic homeostasis in WAT, thus providing potential therapy for obesity and diabetes.

Obesity induces low-grade chronic inflammation in white adipose tissue (WAT) that leads to insulin resistance and metabolic syndromes, thus increasing the risk of many life-threatening diseases such as type 2 diabetes, cardiovascular events, and even cancer (1–3). Adipose inflammation is characterized by recruitment and infiltration of immune cells including macrophages and T cells in adipose tissues (4,5). WAT from obese individuals exhibits not only increased number of macrophages, but also polarization of macrophages toward classically activated M1 expressing high levels of inducible nitric oxide synthase (iNOS) and tumor necrosis factor-α (TNF-α), thereby driving insulin resistance. However, in lean WAT, most of resident macrophages are alternatively activated M2 expressing interleukin (IL)-10 and arginase-1 (Arg-1), which facilitate the maintenance of local immune and metabolic homeostasis (4,6–8). Restoring M2 macrophages in obese individuals by various approaches contributes to the resolution of associated inflammation and insulin resistance (9,10). Emerging evidence has shown the direct involvement of M2 macrophages in metabolic homeostasis. Recent studies have reported that the occurrence of brown-like fats, so-called beiging in WAT, protects against obesity, diabete, and metabolic diseases (11–13). Interestingly, M2 macrophages have been found to release catecholamine to activate the expression of brown adipose tissue–specific uncoupling protein 1 (UCP1) in WAT, thereby promoting beiging and fat burning to dissipate extra energy (14,15).

Adipose-derived stem cells (ADSCs), also known as adipose-derived stromal cells, are mesenchymal stem cells (MSCs) in the stromal vascular fraction (SVF) of adipose tissues. ADSCs possess multipotency to differentiate into different types of cells such as adipocytes, chondrocytes, and osteoblasts. Besides potential application in tissue repair and regeneration, ADSCs have great capacity for immune regulation, as evidenced by controlling inflammatory or autoimmune diseases including

[1]Department of Immunology and Key Laboratory of Infection and Immunity of Shandong Province, School of Basic Medical Sciences, Shandong University, Jinan, Shandong, China
[2]School of Environmental Science and Engineering, Shandong University, Jinan, Shandong, China
Corresponding author: Qun Wang, wangqun@sdu.edu.cn.

Received 22 March 2017 and accepted 4 November 2017.
This article contains Supplementary Data online at http://diabetes.diabetesjournals.org/lookup/suppl/doi:10.2337/db17-0356/-/DC1.

H. Zhao and Q.S. contributed equally to this work.

arthritis, colitis, and autoimmune diabetes (16–20). Previously, we have shown the critical roles of ADSCs in resolution of obesity-associated inflammation and metabolic disorders. ADSCs from visceral WAT-polarized macrophages toward anti-inflammatory M2-like phenotypes, thus remodeling the immune and metabolic homeostasis in WAT. Soluble factors secreted from ADSCs appeared to dominate the polarization of M2 macrophages (21). However, underlying mechanisms for the cross talk between ADSCs and macrophages remain to be unveiled.

Exosomes are nanovesicles derived from multivesicular endosomes and secreted by the cells. In addition to exosome-associated markers like TSG101, CD9, CD63, and CD81, exosomes bear various biological molecules including proteins, lipids, and RNAs. Through transporting these cargos between different types of cells, exosomes mediate intercellular communication and affect both physiological and pathological conditions (22–24). MSCs have been recognized as mass producers of exosomes. As an extension of MSCs' biological roles, exosomes function in bioenergetics, cell proliferation, and immunomodulation, acting in both immediate and remote areas in a paracrine or endocrine manner (25,26). For instance, bone marrow MSC-derived exosomes led to a reduction of myocardial ischemia/reperfusion injury (IRI) in animal models (25,27), and a combination of adipose-derived MSCs and their exosomes protected kidney from acute IRI (28). Therefore, it is of great interest to explore the potential roles of ADSC-derived exosomes in obesity, adipose inflammation, and metabolic disorders.

In this study, we revealed that ADSCs from epididymal WAT secreted exosomes to polarize macrophages toward M2 expressing high levels of Arg-1 and IL-10, which was mainly dependent on active STAT3 transferred by exosomes. Notably, obese mice treated with ADSC-derived exosomes exhibited reduced WAT inflammation, improved metabolic homeostasis, and resistance to obesity progression. ADSC-derived exosomes drove M2 macrophage polarization in WAT, which further promoted WAT beiging, thereby leading to the above beneficial effects.

RESEARCH DESIGN AND METHODS

Animals and Diets

C57BL/6 male mice were provided by Vital River Laboratory Animal Technology Co. Ltd. (Beijing, China). Diets were purchased from Trophic Animal Feed High-tech Co. (Nantong, China). After 1 week of diet adaptation, mice at the age of 8 weeks were fed on a high-fat diet (HFD; 60% of total calories) for 20–26 weeks to induce obesity; mice fed a normal chow diet (NCD) were used as lean controls. Animal studies were approved by Ethics Committee of Shandong University. All procedures were in accordance with the institutional guidelines for animal care and utilization.

Cell Culture

Mouse ADSCs were isolated and cultured as previously described (21). Briefly, epididymal fat pads were obtained from C57BL/6 male mice at the age of 10–12 weeks; SVF was isolated by digestion using type I collagenase (2 mg/mL; Worthington, Lakewood, NJ). After overnight incubation, the adherent stem cell fraction was cultured in complete DMEM containing 10% FBS (Gibco; Invitrogen, Carlsbad, CA) and 5 ng/mL basic fibroblast growth factor (PeproTech, Rocky Hill, NJ). ADSCs at the fourth passage were used for the experiments. Peritoneal macrophages were isolated from C57BL/6 male mice, which were injected with 6% sterile starch solution 3 days previously. After overnight incubation in complete DMEM containing 10% FBS, the adherent cells were used as macrophages.

Isolation of ADSC-Derived Exosomes

ADSCs were cultured with complete DMEM containing 10% FBS (depletion of exosomes by ultracentrifugation) for 2 days (29,30), the supernatants were filtrated through 0.22-μm filters followed by concentrating in 100 K MWCO Amicon Ultra-15 Centrifugal Filter Devices (Merck Millipore, Burlington, MA). Exosomes were isolated from the supernatants using Exoquick-TC (System Biosciences, Mountain View, CA) according to the manufacturer's instruction (30,31) and were characterized by Zetasizer Nano ZSP (Malvern Instruments, Malvern, U.K.), transmission electron microscopy (JEOL Ltd., Tokyo, Japan), and Western blot. In some experiments, exosomes were isolated from ADSCs in which STAT3 activation was inhibited using 20 μmol/L cryptotanshinone (Selleck Chemicals, Houston, TX).

Exosome Transfer Between ADSCs and Macrophages

ADSCs and macrophages were labeled with Vybrant DiO or DiD cell-labeling solution (DiO or DiD; Molecular Probes, Waltham, MA), respectively, and then were cocultured for 30 h; in some experiments, ADSCs labeled with DiO were cocultured with macrophages for 30 h and then were stained with F4/80 using PE-Cy5–conjugated monoclonal antibody (15–4801; eBioscience, San Diego, CA). The fluorescence signals were detected using fluorescence microscope (Carl Zeiss Jena, Jena, Germany) or imaging flow cytometry (ImageStream Mark II; Amnis, Burlington, MA). To detect the direct transfer of exosomes into macrophages, ADSC-derived exosomes were labeled using the PKH67 Fluorescent Cell Linker Kit (PKH67; Sigma-Aldrich, St. Louis, MO) and incubated with macrophages for 24 h, and then the fluorescence signals were detected.

Treatment of Macrophages With ADSC-Derived Exosomes

Macrophages were stimulated with ADSC-derived exosomes (10 and 20 μg/mL) for the indicated time periods, the doses of exosomes were determined according to previous studies with minor modification (32,33). To induce M1 polarization, macrophages were treated with 50 ng/mL lipopolysaccharide (LPS; Sigma-Aldrich) plus 20 ng/mL interferon-γ (IFN-γ; PeproTech). In some experiments, STAT3 was silenced in macrophages by transfection with STAT3 siRNA (siSTAT3; Sigma-Aldrich) using Jet-PRIME (Polyplus, Berkeley, CA) before the addition of exosomes. The siSTAT3 sequences are listed in Supplementary Table 1.

Treatment With ADSC-Derived Exosomes in HFD-Fed Mice

During the last 6–8 weeks of HFD feeding, mice were intraperitoneally administrated with ADSC-derived exosomes (30 μg/mouse, once every 3 days) according to previous studies with minor modification (32,34); HFD or NCD-fed mice treated with normal saline (NS) were used as controls. Body weight and food intake were evaluated during the intervention. After the intervention, mice were sacrificed under anesthesia. Serum, liver, and adipose tissues were collected. In exosome-tracking experiments, ADSC-derived exosomes (50 μg/mouse) were labeled with PKH67 and delivered into HFD-fed mice by intraperitoneal injection. After 24 h, the epididymal fat pads were harvested to detect fluorescence signals.

Measurement of Metabolic Parameters

Serum triglyceride (TG) and total cholesterol (TC) were detected after the intervention using commercial kits (Nanjing Jiancheng Bioengineering Institute, Nanjing, China). Glucose tolerance test (GTT) and insulin tolerance test (ITT) were conducted after 5 or 6 weeks of intervention, respectively. GTT was performed in mice following an overnight fast; blood glucose levels were determined at different time points after intraperitoneal injection of glucose (2 g/kg body weight; Sigma-Aldrich). ITT was performed in mice with free access to food and water; blood glucose levels were examined at different time points after intraperitoneal administration of human insulin (0.75 units/kg body weight; Wanbang, Xuzhou, China).

Flow Cytometry

SVF from epididymal adipose tissues was stained with PE-Cy5–conjugated monoclonal antibody against mouse F4/80 (15–4801; eBioscience) followed by intracellular staining with fluorescein-conjugated Ab against mouse Arg-1 (IC5868F; R&D Systems, Minneapolis, MN), using isotypic antibodies as controls. Fc block was used prior to staining. Cells were acquired using Cytomics FC500 (Beckman Coulter, Pasadena, CA).

Statistical Analysis

Data were expressed as mean ± SEM. Statistical differences were evaluated using Student *t* test or one- or two-way ANOVA. A P value <0.05 was considered significant.

RESULTS

Exosomes Transfer From ADSCs to Macrophages

Previously, we have shown that ADSCs induced macrophage polarization toward M2-like phenotypes (21). To elucidate the roles of exosomes in ADSC–macrophage cross talk, ADSCs and macrophages were labeled with DiO or DiD and cocultured to detect exosome transfer as described previously (35). Interestingly, we found that exosomes transferred between macrophages but not ADSCs. However, in the coculture of ADSCs and macrophages, unidirectional transfer of exosomes from ADSCs to macrophages was observed (Fig. 1*A*). Imaging flow cytometry confirmed that macrophages (DiD^+ or $F4/80^+$) displayed green fluorescence from ADSCs (DiO^+) after coculture, indicating exosome transfer from ADSCs to macrophages (Fig. 1*B*). Furthermore, exosomes from ADSCs were collected, which were ~100 nm in diameter, cup-shaped, and positive for exosomal markers TSG101, CD9, CD63, and HSP90 (Fig. 1*C–E*). After labeled with PKH67 and incubated with macrophages, ADSC-derived exosomes with green fluorescence were observed in macrophages (Fig. 1*F*), suggesting the uptake of exosomes by macrophages.

ADSC-Derived Exosomes Induce M2 Macrophage Polarization

Next, the effects of ADSC-derived exosomes on macrophage polarization were analyzed. Macrophages educated by ADSC-derived exosomes showed remarkable increases in mRNA levels of M2-related *Arg-1* and *IL-10*, but no significant changes in those of M1-related *iNOS*, *TNF-α*, and *IL-12*; these phenotypes were different from M1 macrophages induced by LPS plus IFN-γ, which expressed high levels of *iNOS*, *TNF-α*, and *IL-12* mRNA (Fig. 2*A–E*). The increase of Arg-1 in macrophages induced by exosomes was substantiated on protein levels in a dose-dependent manner (Fig. 2*F*). In addition, preincubation with ADSC-derived exosomes obviously mitigated inflammatory responses of macrophages stimulated by LPS plus IFN-γ, as evidenced by marked decreases in levels of *iNOS*, TNF-α, and IL-12 (Fig. 2*G–K*). These data indicate that ADSC-derived exosomes induce macrophage polarization toward M2 phenotypes, thus reducing the ability of macrophages to evoke inflammatory responses.

ADSC-Derived Exosomes Attenuate Diet-Induced Obesity and Metabolic Disorders in HFD-Fed Mice

Considering the beneficial roles of ADSC-derived exosomes in M2 polarization, we further detected their effects on obesity and associated metabolic disorders. Administration of ADSC-derived exosomes led to a resistance to sustained weight gain in HFD-fed mice during the later period of intervention (Fig. 3*A* and *B*), which was independent of food intake (Supplementary Fig. 1). For both visceral and subcutaneous white fat pads, HFD feeding caused dramatic increases in the percentages of fat weight to body weight, whereas exosome treatment significantly decreased these percentages (Fig. 3*C* and Supplementary Fig. 2). Importantly, HFD-fed mice treated with ADSC-derived exosomes showed significant improvement in glucose tolerance and insulin sensitivity even before the reduction in obesity progression (Fig. 3*D–G*). In addition, treatment with ADSC-derived exosomes decreased the levels of TG and TC in serum of HFD-fed mice (Fig. 3*H* and *I*). The hepatic steatosis in HFD-fed mice was also attenuated by exosome delivery, manifested by significant reductions in liver weight, macrovesicular steatosis, and levels of hepatic TG (Fig. 3*J–L* and Supplementary Fig. 3). These data indicate the pivotal roles of ADSC-derived exosomes in obesity resistance and metabolic improvement.

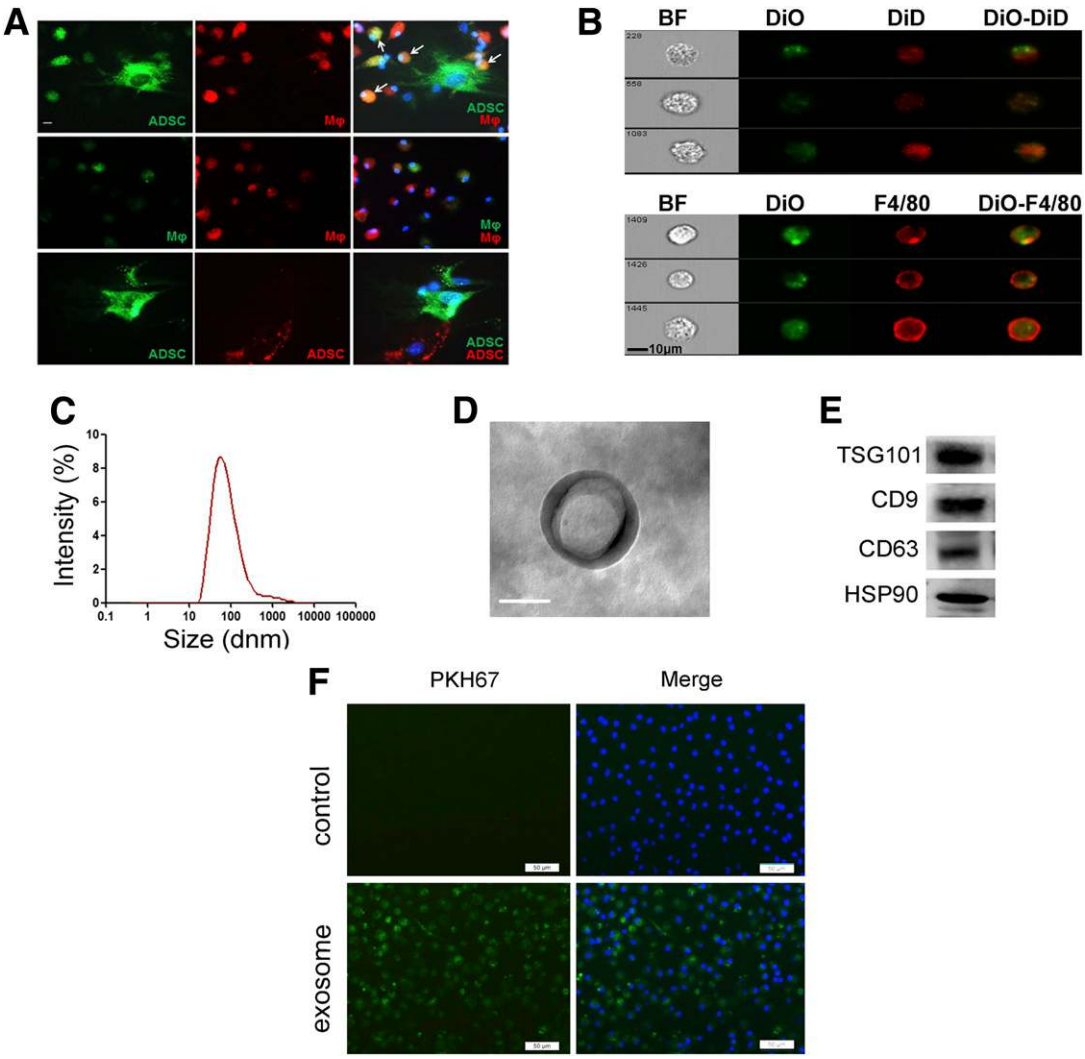

Figure 1—Exosomes transfer from ADSCs to macrophages. *A*: Epididymal fat-derived ADSCs or peritoneal macrophages (Mφ) from lean C57BL/6 mice were labeled with DiO (green) or DiD (red) in monoculture and then were cocultured for 30 h; fluorescence signals were detected by fluorescence microscope. White arrows indicate exosome transfer from ADSCs to macrophages. Scale bar: 20 μm. *B*: After 30 h of coculture with ADSCs (DiO^+), macrophages (DiD^+ or $F4/80^+$) were detected for fluorescence signals by imaging flow cytometry (bright field [BF]). Scale bar: 10 μm. Exosomes from mice ADSCs were identified by Zetasizer Nano ZSP (*C*), transmission electron microscope (scale bar: 50 nm) (*D*), and Western blot (*E*). *F*: ADSC-derived exosomes were labeled with PKH67 and cocultured with macrophages for 24 h; fluorescence signals were examined by fluorescence microscope. Scale bars: 50 μm. Data are representative of at least two independent experiments.

ADSC-Derived Exosomes Inhibit Adipocyte Hypertrophy and Promote WAT Beiging in HFD-Fed Mice

To determine the direct impact of ADSC-derived exosomes on WAT, we tracked PKH67-labeled exosomes in HFD-fed mice after intraperitoneal administration and found that ADSC-derived exosomes with green fluorescence successfully settled in epididymal fat pads (Supplementary Fig. 4). Compared with NCD-fed mice, HFD-fed obese mice showed adipocyte hypertrophy in epididymal and inguinal WAT, whereas successive administration of ADSC-derived exosomes in HFD-fed obese mice significantly mitigated adipocyte hypertrophy in both fat depots, as confirmed by decreases in adipocyte size and leptin expression in both epididymal and inguinal WAT (Fig. 4*A*–*C*). Thus, ADSC-derived exosomes effectively inhibited adipocyte hypertrophy and favored WAT homeostasis.

Considering the contribution of beiging in energy balance and WAT homeostasis, we further detected the gene expression related to brown and beige adipocytes (*UCP1*, peroxisome proliferator–activated receptor γ coactivator α [*PGC1α*], *PRDM16*, *CIDEA*, *TBX1*, and *TMEM26*) and mitochondrial fatty acid oxidation (*PGC1β*, *CPT1α*, and *CPT1β*) in both epididymal and inguinal WAT. Compared with NCD feeding, long-term HFD feeding broadly inhibited the expression of these genes in epididymal WAT, whereas administration of ADSC-derived exosomes significantly reversed their expression. As for inguinal WAT, deliveries of ADSC-derived exosomes dramatically increased the expression of most of the above genes, particularly brown adipocyte-related *UCP1*, *PGC1α*, and beige adipocyte-related *TBX1* and *TMEM26* (Fig. 4*D*–*F* and Supplementary Fig. 5).

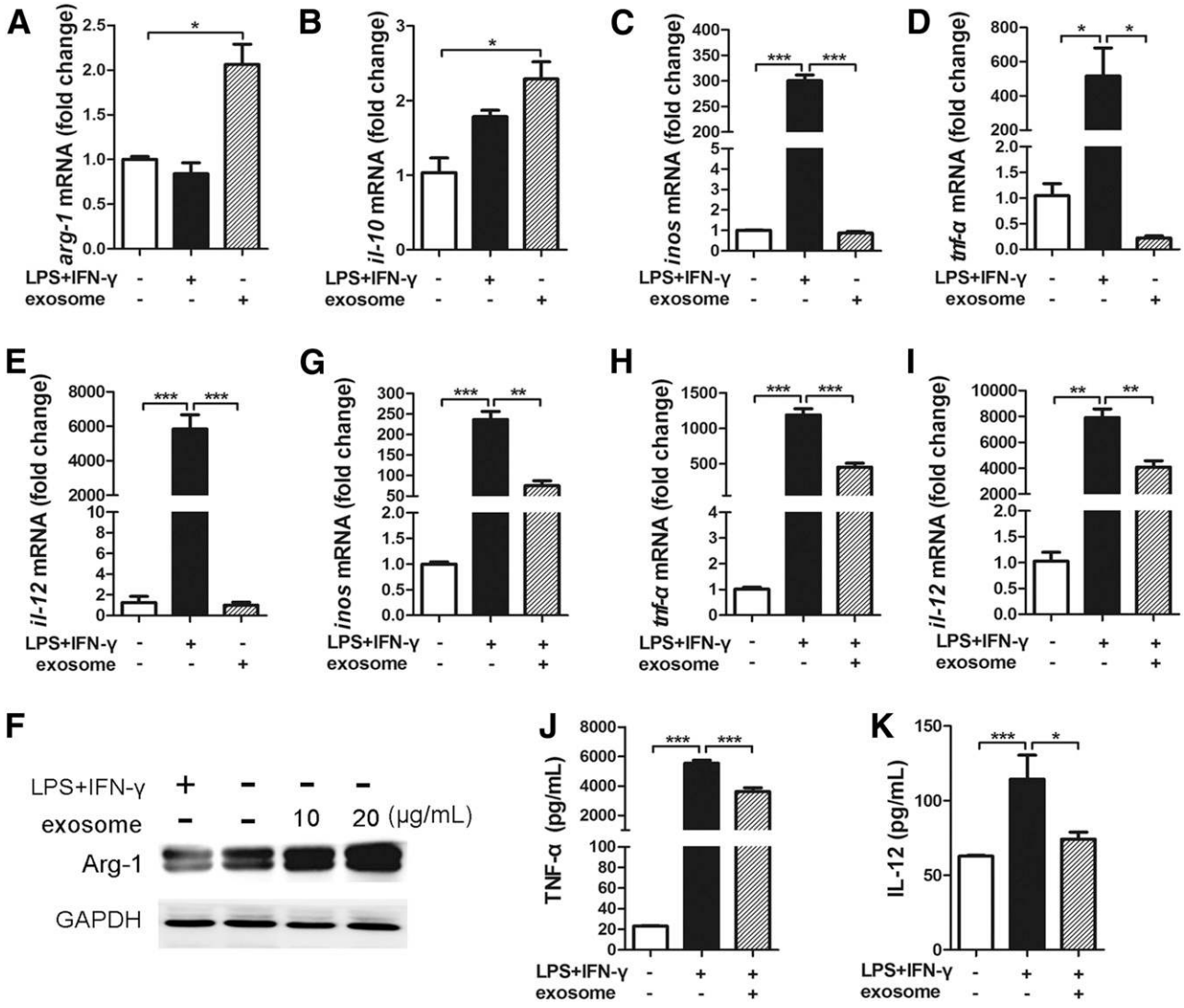

Figure 2—ADSC-derived exosomes induce M2 polarization. Macrophages were treated with ADSC-derived exosomes (20 μg/mL in *A–E*; 10 and 20 μg/mL in *F*) for 30 h or LPS (50 ng/mL) plus IFN-γ (20 ng/mL) for 6 h. The mRNA levels of M2-related *arg-1* (*A*) and *il-10* (*B*) and M1-related *inos* (*C*), *tnf-α* (*D*), and *il-12* (*E*) were determined by quantitative PCR (qPCR); the protein levels of Arg-1 were detected by Western blot (*F*). Macrophages were treated with ADSC-derived exosomes (20 μg/mL) for 30 h and then were stimulated with LPS (50 ng/mL) plus IFN-γ (20 ng/mL) during the last 2 h (for qPCR in *G–I*) or 6 h (for ELISA in *J* and *K*). The mRNA levels of *inos* (*G*), *tnf-α* (*H*), and *il-12* (*I*) were detected by qPCR. The secretion of TNF-α (*J*) and IL-12 (*K*) was examined by ELISA. Data are representative of at least three independent experiments and presented as mean ± SEM of three replicates (*A–E* and *G–I*). *J* and *K* show pooled data from three independent experiments. $^{*}P < 0.05$; $^{**}P < 0.01$; $^{***}P < 0.001$ determined by one-way ANOVA with Bonferroni comparisons.

Consistently, the protein levels of UCP1 suppressed by HFD feeding were restored in epididymal WAT and elevated in inguinal WAT by ADSC-derived exosomes (Fig. 4*G*). These data indicate that ADSC-derived exosomes promote WAT beiging and restore UCP1-dependent energy expenditure, which are blunted by HFD feeding.

ADSC-Derived Exosomes Ameliorate WAT Inflammation in HFD-Fed Mice Through Remodeling Macrophage Phenotypes

WAT inflammation is associated with WAT dysfunction and metabolic disorders. To delineate the mechanism by which ADSC-derived exosomes favored WAT homeostasis, WAT inflammation was detected. As expected, administration of ADSC-derived exosomes in HFD-fed mice significantly reduced the secretion of proinflammatory TNF-α, but increased that of anti-inflammatory IL-10 from epididymal adipose explants (Fig. 5*A* and *B*). To verify the effects of ADSC-derived exosomes on adipose tissue macrophages, we further analyzed the expression of M1- or M2-related genes on SVF. The mRNA levels of *TNF-α*, *IL-12*, and *IL-6*, which were also M1 phenotypes induced by obesity, were significantly decreased in SVF from HFD-fed mice treated with ADSC-derived exosomes. Notably, exosome delivery into HFD-fed mice led to a dramatic increase in mRNA levels of *Arg-1*, a representative M2 phenotype in SVF (Fig. 5*C*). Flow cytometry analysis showed that the infiltration of

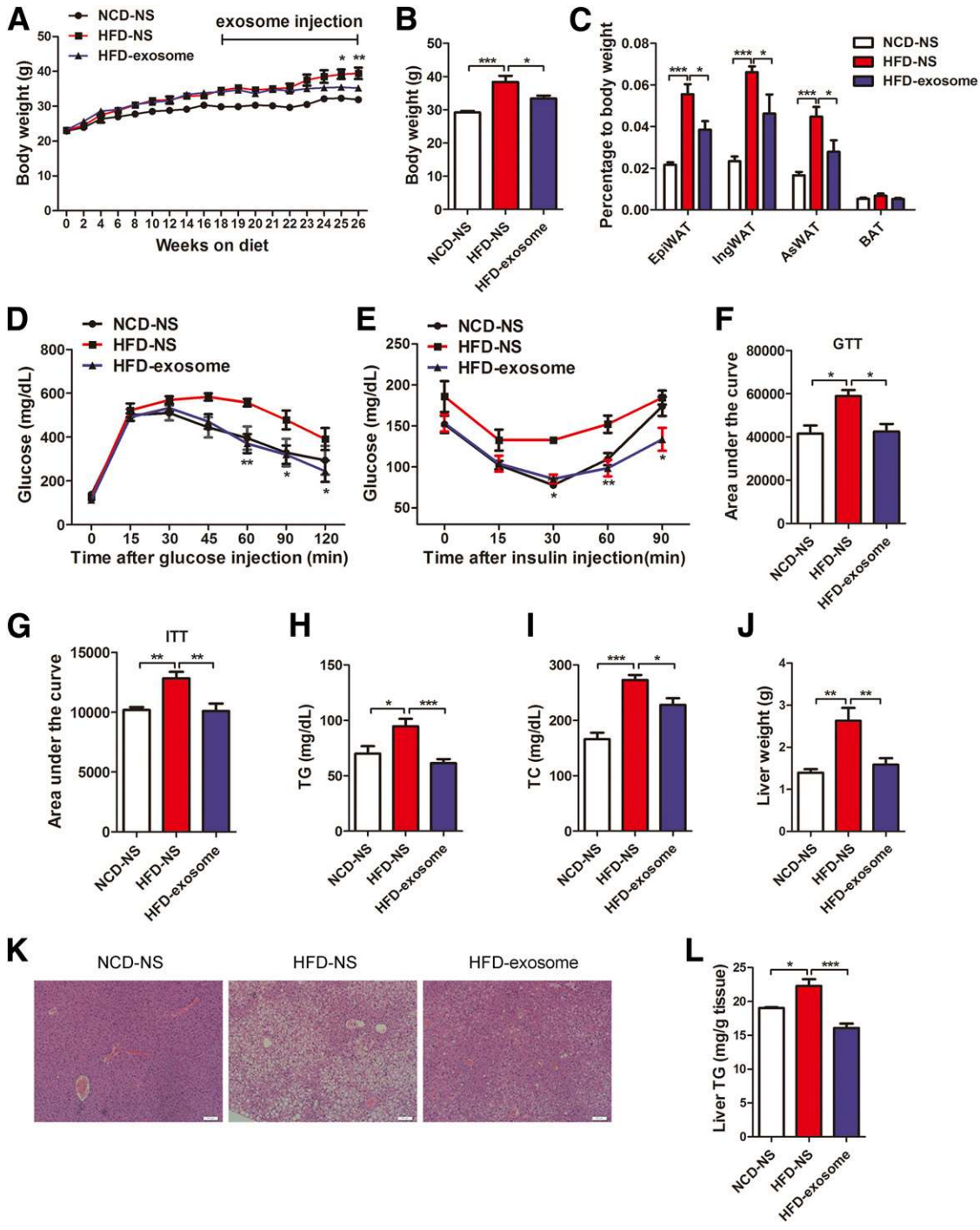

Figure 3—Delivery of ADSC-derived exosomes attenuates obesity and metabolic disorders in HFD-fed mice. *A–L*: C57BL/6 male mice were fed NCD or HFD for 20–26 weeks. HFD-fed mice were intraperitoneally injected with ADSC-derived exosomes (30 μg per mice, once every 3 days) during the last 6–8 weeks; NCD or HFD-fed mice treated with NS were used as controls. Body weight change (*A*) during the experiment and body weight (*B*) after the intervention (n = 5 to 6 mice/group) were evaluated. Percentages of fat weight to body weight (*C*) after the intervention (n = 4–6 mice/group) were determined (epididymal WAT [EpiWAT], inguinal WAT [IngWAT], anterior subcutaneous WAT [AsWAT], and brown adipose tissue [BAT]). GTT (*D*) and ITT (*E*) were performed in mice (n = 4–6/group) after 5 or 6 weeks of intervention, respectively. Values of area under the curve in GTT (*F*) and ITT (*G*) were measured. After the intervention, serum TG (*H*) and TC (*I*) (n = 10–16 mice/group) were detected; liver weight (*J*), hematoxylin and eosin staining (*K*) for liver tissues, and hepatic TG levels (*L*) were determined (n = 4–6 mice/group). Scale bars: 50 μm. $^*P < 0.05$; $^{**}P < 0.01$; $^{***}P < 0.001$ determined by two-way (HFD-NS versus HFD-exosome) or one-way ANOVA.

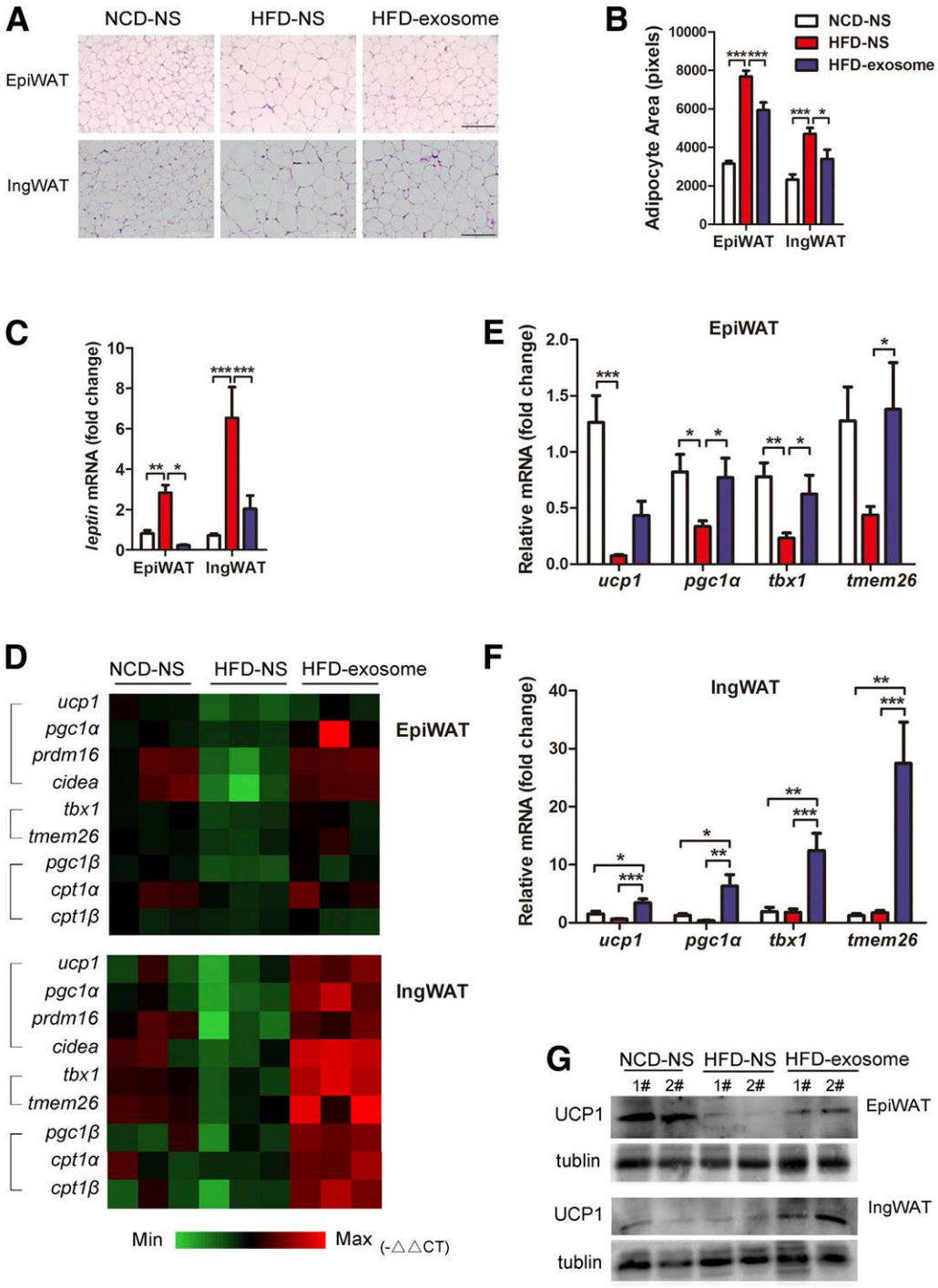

Figure 4—ADSC-derived exosomes improve WAT homeostasis in HFD-fed mice. Mice (n = 3–6/group) were treated as described in Fig. 3; epididymal and inguinal adipose tissues were collected for assay. Hematoxylin and eosin staining (*A*) (scale bars: 200 μm) was performed. Average adipocyte size (*B*) was presented as pixels. The mRNA levels of *leptin* (*C*) were detected. Heat map (*D*) and relative mRNA levels (*E* and *F*) of gene expression related to brown or beige adipocyte and mitochondrial fatty acid oxidation in epididymal WAT (EpiWAT) and inguinal WAT (IngWAT) were determined. Protein levels of UCP1 (*G*) were detected in EpiWAT and IngWAT by Western blot. $^*P < 0.05$; $^{**}P < 0.01$; $^{***}P < 0.001$ determined by one-way ANOVA with Bonferroni comparisons.

F4/80$^+$ macrophages in WAT from HFD-fed obese mice significantly decreased after exosome treatment (Fig. 5*D–F*). More exciting, compared with HFD-fed obese mice or NCD-fed lean mice, exosome-treated HFD-fed mice showed significantly elevated expression of Arg-1 on macrophages in WAT (Fig. 5*G–I*), confirming the critical role of ADSC-derived exosomes in driving adipose macrophage polarization toward Arg-1^{high} M2. Altogether, these data suggest

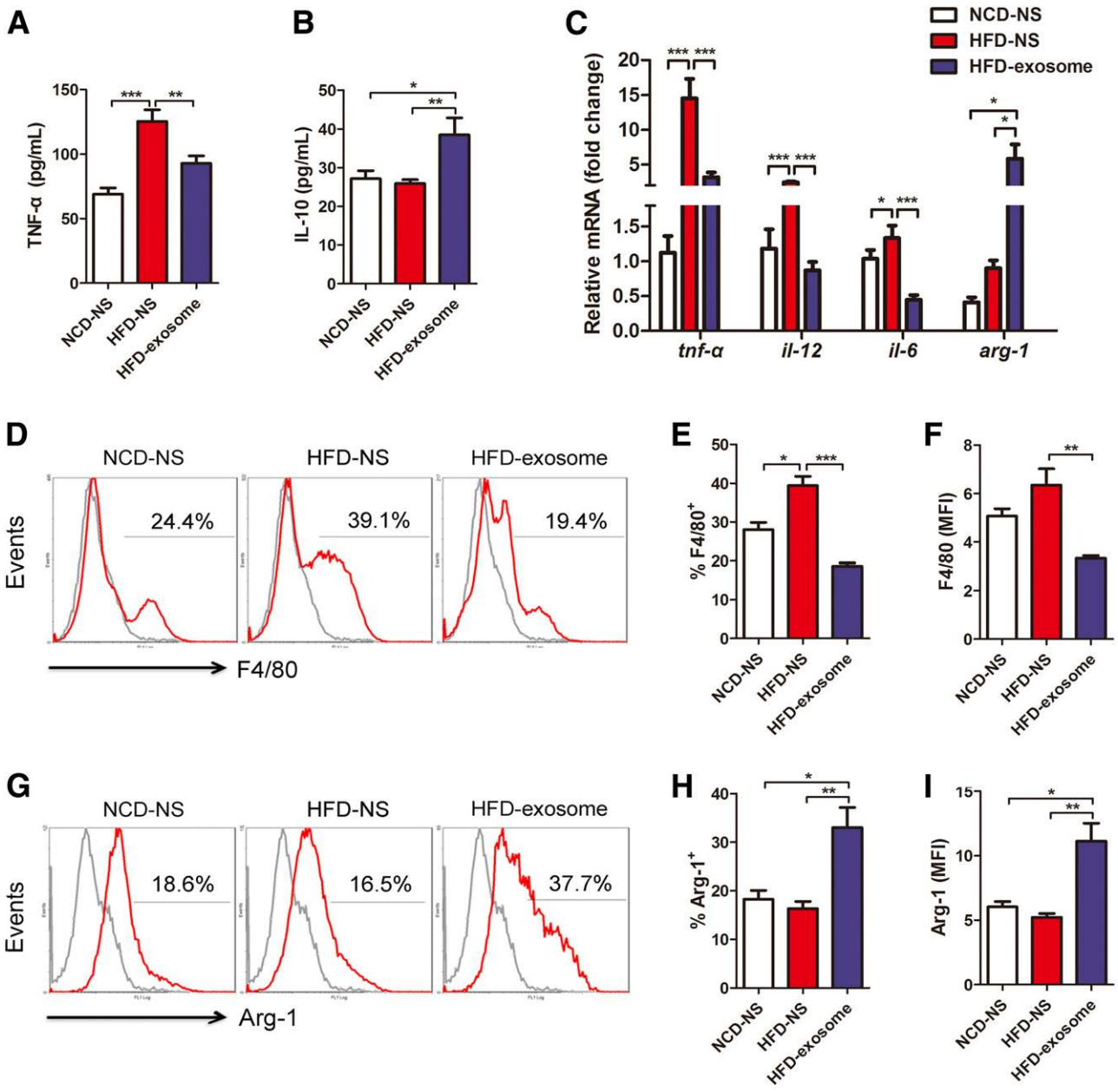

Figure 5—ADSC-derived exosomes ameliorate WAT inflammation in HFD-fed mice through remodeling macrophage phenotypes. Mice were treated as described in Fig. 3. Secretion levels of TNF-α (*A*) and IL-10 (*B*) from epididymal adipose tissue explants (n = 4–6 mice/group) were detected using ELISA. The mRNA levels of M1- or M2-related genes (*C*) in SVF from epididymal WAT (n = 4–6 mice/group) were detected. The expression of F4/80 (*D–F*) in SVF and the expression of Arg-1 (*G–I*) in F4/80$^+$ SVF from epididymal WAT (n = 3 mice/group) were analyzed by flow cytometry. *$P < 0.05$; **$P < 0.01$; ***$P < 0.001$ determined by one-way ANOVA with Bonferroni comparisons.

that ADSC-derived exosomes reduce WAT inflammation through reprograming adipose macrophages from M1 to Arg-1^{high} M2 subtype.

ADSC-Derived Exosomes Drive Arg-1 Expression Through Transporting STAT3

In macrophages educated by ADSC-derived exosomes, the elevation of Arg-1 was accompanied by enhanced STAT3 phosphorylation in a dose-dependent manner (Fig. 6*A*). Considering the expression levels of total STAT3 were also increased in macrophages upon exosome stimulation, we speculated that STAT3 might be carried into macrophages by exosomes. Actually, the presence of STAT3 in phosphorylated form was observed in both ADSC-derived exosomes and their parental ADSCs (Fig. 6*B*). Next, exosomes were obtained from ADSCs in which STAT3 phosphorylation was inhibited using cryptotanshinone (Fig. 6*C* and *D*). The phosphorylation of STAT3 was greatly decreased in macrophages treated with exosomes carrying

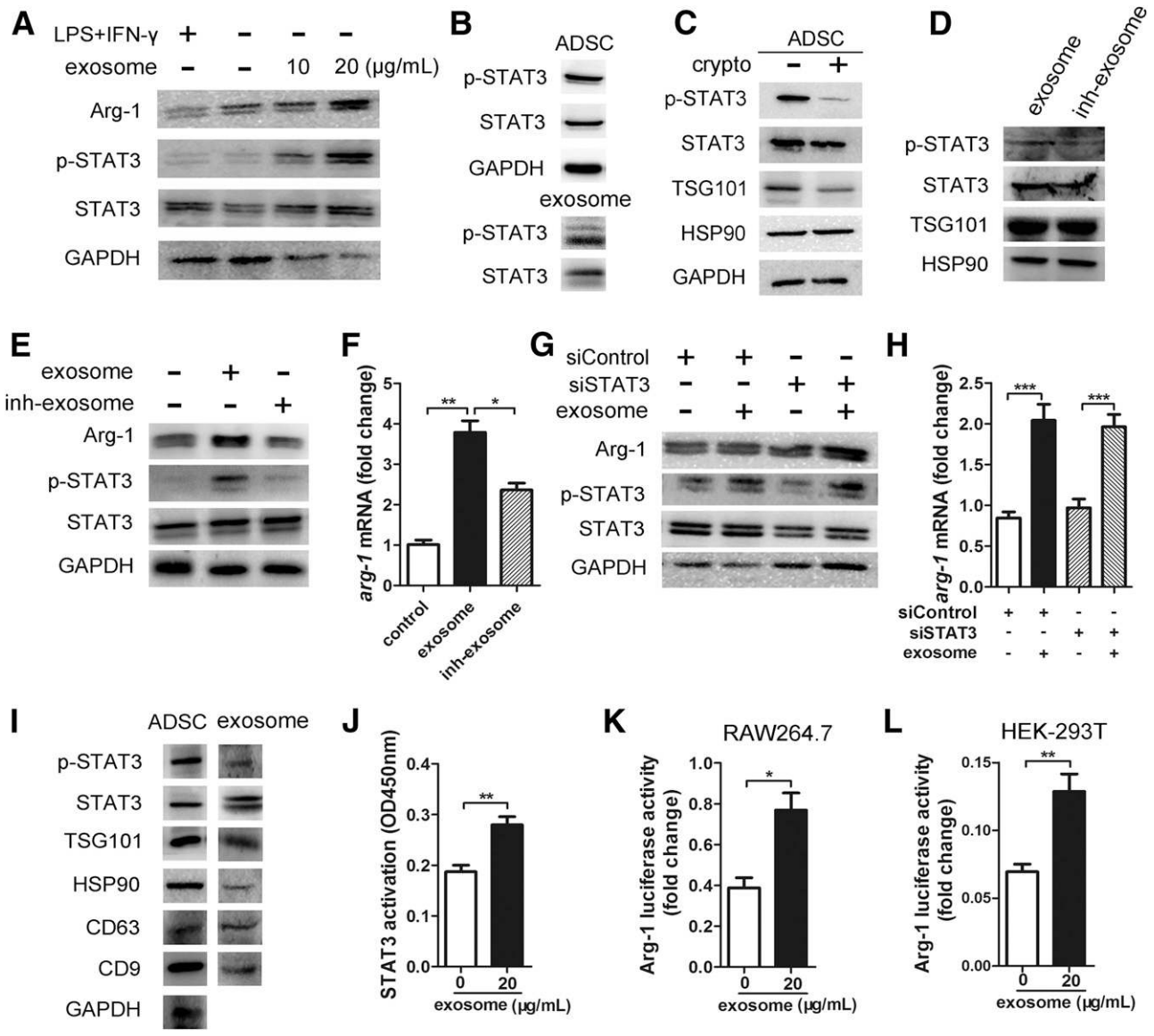

Figure 6—ADSC-derived exosomes drive the expression of Arg-1 through transporting active STAT3. *A*: Macrophages were treated with ADSC-derived exosomes or LPS plus IFN-γ as in Fig. 2*A–E*; the expression of Arg-1, p-STAT3, and STAT3 in macrophages was detected by Western blot. *B*: The expression of p-STAT3 and STAT3 was detected in both ADSCs and ADSC-derived exosomes by Western blot. *C–F*: After treatment with STAT3 inhibitor cryptotanshinone (crypto; 20 μmol/L) for 48 h, ADSCs (*C*) and ADSC-derived exosomes (*D*) were detected for the expression of p-STAT3, STAT3, and exosomal markers. Macrophages were stimulated with exosomes from ADSCs treated with crypto; the expression of Arg-1, p-STAT3, and STAT3 was detected by Western blot (*E*) and quantitative PCR (*F*). *G* and *H*: Macrophages with silenced STAT3 via siRNA were stimulated with ADSC-derived exosomes; the expression of Arg-1, p-STAT3, and STAT3 was detected by Western blot (*G*) and quantitative PCR (*H*) (siSTAT3 and control siRNA [siControl]). *I* and *J*: Exosomes from human ADSCs were identified for p-STAT3, STAT3, and exosomal markers (*I*); the active form of STAT3 in exosomes was determined using DNA-binding ELISA (*J*). *K–L*: After transfection with pGL3-mArg1 promoter/enhancer and pRL-TK-Renilla-luciferase, RAW264.7 (*K*) and HEK-293T (*L*) were stimulated with ADSC-derived exosomes for 24 h. Luciferase activities were measured with Dual Luciferase Reporter Assay. Data are representative of more than three independent experiments and shown as mean ± SEM of three (*F* and *H*) or at least four (*K* and *L*) replicates. *J* shows pooled data from three experiments. $^*P < 0.05$; $^{**}P < 0.01$; $^{***}P < 0.001$ determined by one-way ANOVA or Student *t* test. ihn-exosome, exosome from ADSC treated with STAT3 inhibitor; OD, optical density.

hypophosphorylated STAT3, compared with those treated with normal exosomes (Fig. 6*E*); more importantly, an obvious reduction in Arg-1 expression was observed in these macrophages on both mRNA and protein levels (Fig. 6*E* and *F*). In contrast, knockdown of STAT3 in macrophages had no significant impact on the elevation of phosphorylated (p-)STAT3 and Arg-1 caused by ADSC-derived exosomes (Fig. 6*G* and *H*), indicating that p-STAT3 carried by ADSC-derived exosomes dominated the induction of Arg-1 in macrophages.

It has been reported that active STAT3 binds to the promoter region of human *Arg-1* and enhances its expression and activity (36). To examine the transactivation activity of p-STAT3 from ADSC-derived exosomes on Arg-1

expression, we purified exosomes from human ADSCs, which expressed similar exosomal markers to those from mice and also carried p-STAT3 (Fig. 6*I*), and verified their capacity to bind consensus target DNA of STAT3 (Fig. 6*J*). Furthermore, exosomes from mice ADSCs were taken up and significantly enhanced the transcriptional activity of *Arg-1* promoter/enhancer in both RAW264.7 and HEK-293T cells (Supplementary Fig. 6 and Fig. 6*K* and *L*). These data demonstrate that STAT3 in ADSC-derived exosomes is active and functional, which is able to directly promote the expression of Arg-1 in recipient cells.

Macrophages Educated by ADSC-Derived Exosomes Promote ADSC Proliferation and Highly Express Tyrosine Hydroxylase

High arginase activity contributes to synthesis and release of polyamines, which promote cell proliferation (37,38). To determine the effects of Arg-1^{high} M2 macrophages on WAT homeostasis, we cocultured ADSCs with conditional medium (CM) from Arg-1^{high} M2 macrophages, which were induced by ADSC-derived exosomes. The proliferation curves showed that CM from Arg-1^{high} M2 promoted the proliferation of ADSCs (Fig. 7*A*). 5-Ethynyl-2′-deoxyuridine (EdU) incorporation assay also revealed that CM from Arg-1^{high} M2 drove more ADSCs entering EdU^{+} S phase (Fig. 7*B* and *C*), suggesting the contribution of Arg-1^{high} M2 to ADSC proliferation and self-renewal.

Lactate plays an important role in browning of white adipose cells (39). Interestingly, we detected higher levels of lactate in ADSC culture upon treatment with CM from Arg-1^{high} M2 (Fig. 7*D*), whereas there was no difference in lactate levels in CM from macrophages in the absence or presence of exosomes (Fig. 7*E*). This could be due to the contribution of ADSC proliferation to lactate production via anaerobic glycolysis, and lactate produced by proliferating ADSCs might be an important contributor to UCP1 expression and WAT beiging. In addition, Arg-1^{high} M2 educated by ADSC-derived exosomes expressed high levels of tyrosine hydroxylase (TH), a rate-limiting enzyme for catecholamine synthesis (Fig. 7*F* and *G*). Accordingly, compared with untreated obese mice, exosome-treated HFD-fed mice had higher levels of *TH* expression in SVF from epididymal WAT (Fig. 7*H*), suggesting catecholamine catalyzed by TH could be another contributor to UCP1 expression and WAT beiging.

DISCUSSION

WAT has been recognized as a complex endocrine organ that serves as a master regulator of systemic energy homeostasis, performing intricate metabolic functions under physiological conditions (40–42). Obesity is associated with unhealthy expansion and dysfunction of WAT that lead to inflammation, insulin resistance, and increased risk for metabolic diseases. Therefore, the potential of targeting WAT in the treatment of obesity and associated diabetes is gaining substantial interest (40). Based on our previous finding showing that ADSCs control obesity-induced WAT inflammation and metabolic disorders (21), in the current study, we propose exosomes as natural messengers for ADSC–macrophage cross talk, which drive M2 polarization and subsequent beiging and metabolic homeostasis in WAT, thereby preventing adipose tissue inflammation, metabolic disorders, hepatic steatosis, and obesity progression.

We demonstrated that ADSCs secreted exosomes to act on macrophages, inducing high levels of M2-related Arg-1 and IL-10 and inhibiting macrophage inflammatory responses stimulated by LPS plus IFN-γ. Different from M2 macrophages induced by IL-4 plus IL-13, which depend on the activation of STAT6 (43,44), Arg-1^{high} M2 induced by ADSC-derived exosomes displayed enhanced levels of p-STAT3. As a crucial biomarker for stem cells, STAT3 was observed in ADSCs. More importantly, p-STAT3 was detected in exosomes released by ADSCs, indicating ADSC-derived exosomes could be an important source of p-STAT3 in recipient macrophages. In fact, exosomes from ADSCs lacking STAT3 activation failed to induce Arg-1 expression in macrophages, whereas knockdown of STAT3 in macrophages had no detectable influence on Arg-1 expression triggered by ADSC-derived exosomes. We further revealed the capacity of ADSC-derived exosomes to bind to STAT3 target DNA and promote the transcriptional activation of *Arg-1* promoter/enhancer, thus confirming that ADSC-derived exosomes induced macrophage polarization toward Arg-1^{high} M2 mainly through transporting the special cargo, active STAT3. It should be noted that our study does not exclude the possibility that some specific microRNAs carried by ADSC-derived exosomes also play a role in regulating the expression of Arg-1 in macrophages, more potential multiple mechanisms by which ADSC-derived exosomes influence macrophages remain to be unveiled.

Emerging evidence has shown the therapeutic roles of exosomes from MSCs in several IRI models based on their function in tissue repair, but few reports have addressed their immunoregulatory role in inflammatory diseases (27,28,45,46). In the current study, the desirable immunomodulation elicited by ADSC-derived exosomes makes it possible to substitute ADSCs in the treatment of obesity-associated inflammation. As expected, deliveries of ADSC-derived exosomes into HFD-fed mice markedly reduced obesity-induced WAT inflammation, systemic insulin resistance, dyslipidemia, and hepatic steatosis. A 27.8% improvement of insulin action was observed in HFD-fed mice treated with exosomes by determining the area under the curve of GTT. These beneficial effects produced by ADSC-derived exosomes were partially consistent with and even superior to the therapeutic effects of ADSCs (21,47). The presence of ADSC-derived exosomes in WAT ensured the direct communication between exosomes and macrophages. Indeed, exosome administration induced a subset of Arg-1^{high} macrophages in WAT of HFD-fed mice, driving a shift of WAT macrophages from proinflammatory M1 phenotypes toward anti-inflammatory M2 phenotypes and leading to the resolution of WAT inflammation and subsequent improvement of systemic metabolic homeostasis. The involvement of MSC-released cytokines like IL-10 in limiting

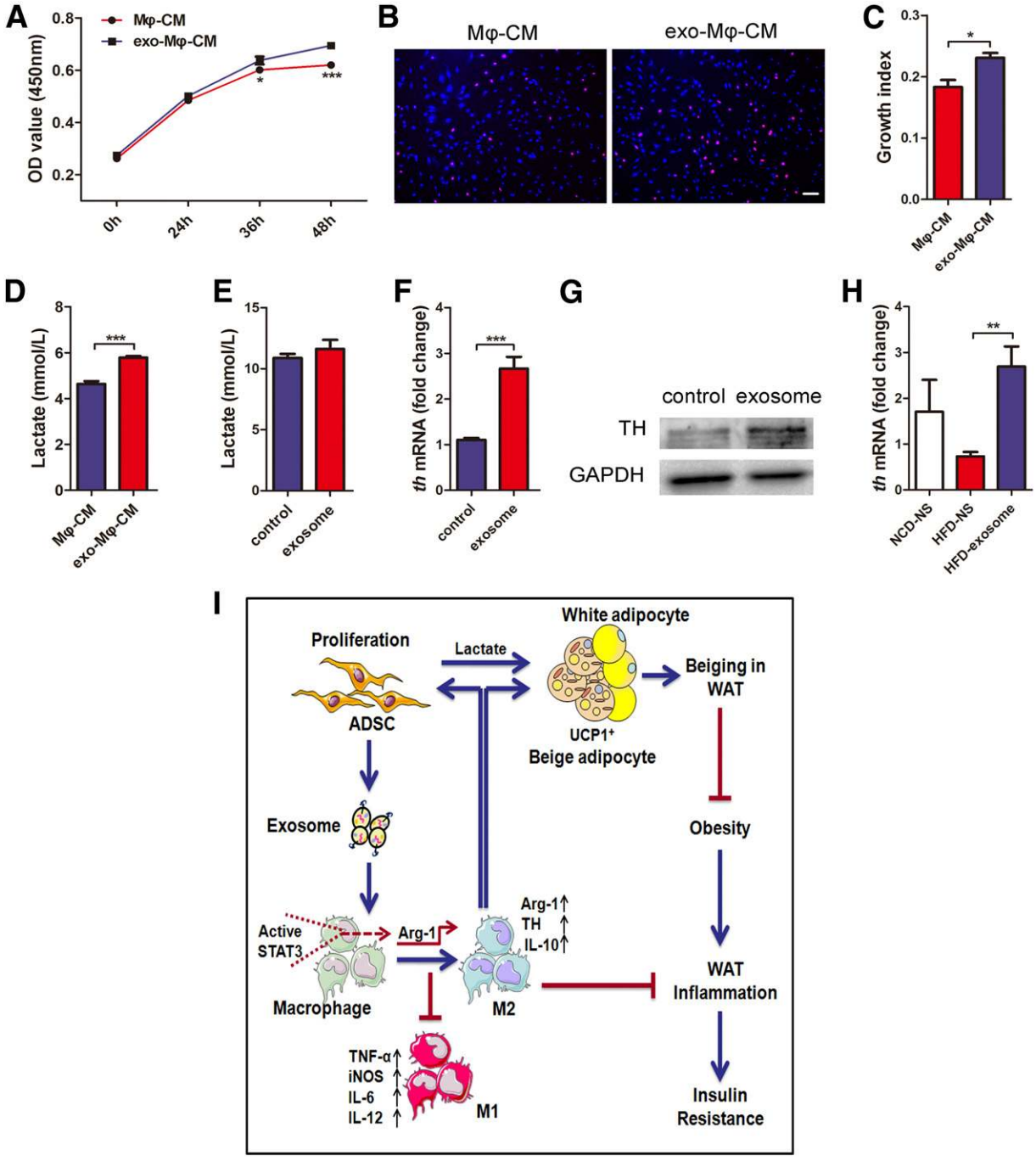

Figure 7—Macrophages (Mφ) educated by ADSC-derived exosomes contribute to ADSC proliferation and express high levels of TH. *A–D*: ADSCs were cultured with CM from macrophages educated by ADSC-derived exosomes for indicated time periods. ADSC proliferation was detected by CCK-8 assay (*A*) and EdU incorporation assay (*B* and *C*). Data are shown as mean ± SEM of five (*A*) or three (*C*) replicates and representative of two independent experiments. Scale bar: 100 μm. Lactate levels (*D*) in supernatants from ADSC culture were determined (CM from macrophages [Mφ-CM]; CM from macrophages educated by ADSC-derived exosomes [exo-Mφ-CM]). *E*: Lactate levels in supernatants from macrophages were determined in the absence or presence of ADSC-derived exosomes. Data are shown as mean ± SEM of six replicates (*D* and *E*) representing two independent experiments. *F* and *G*: Macrophages were treated with ADSC-derived exosomes (20 μg/mL) for 30 h; the mRNA (*F*) and protein (*G*) levels of TH were examined. Data are representative of at least three independent experiments and shown as mean ± SEM of three replicates in *F*. *H*: Mice (n = 4–6/group) were treated as described in Fig. 3; the mRNA levels of *th* were detected in SVF of epididymal WAT. *I*: Working model of ADSC-derived exosomes in polarizing M2 macrophages and inducing WAT beiging. $^{*}P < 0.05$; $^{**}P < 0.01$; $^{***}P < 0.001$ determined by Student t test or two- or one-way ANOVA. OD, optical density.

inflammation and the presence of cytokines in exosomes have been reported (48). We cannot exclude the roles of ADSC-derived cytokines in immunomodulation or the possibility that cytokines in ADSC-derived exosomes act on macrophages. The cooperation of cytokines and exosomes in immunomodulation remains to be investigated.

Besides immune homeostasis, deliveries of ADSC-derived exosomes into HFD-fed mice also facilitated WAT metabolic homeostasis, including reduction in adipocyte hypertrophy and WAT beiging responsible for energy expenditure. Cold-induced M2 macrophages could express TH that catalyzes the production of catecholamine, thereby driving beiging of WAT (14,15). In this study, we showed that macrophages educated by ADSC-derived exosomes also expressed high levels of TH, which might drive WAT beiging and facilitate energy expenditure under the circumstances of long-term HFD. As progenitor cells of adipocytes, ADSCs account for de novo adipogenesis and contribute to the healthy expansion of WAT through adipocyte hyperplasia rather than adipocyte hypertrophy (40). So, ADSC self-renewal and amplification driven by exosome-educated Arg-1^{high} macrophages would be another contributor to WAT metabolic homeostasis. Meanwhile, amounts of lactate from rapidly proliferated ADSCs also contributed to UCP1 expression and WAT beiging in HFD-fed mice treated with ADSC-derived exosomes. Therefore, ADSC-derived exosomes engender beneficial effects on both systemic metabolic improvement and resistance to obesity progression (Fig. 7*I*). Furthermore, exosome treatment in HFD-fed mice also increased the expression of *PGC1α* and *CPT1β* in brown adipose tissue (Supplementary Fig. 7), which could further promote energy expenditure and obesity resistance.

Exosomes possess desirable characteristics like nanometer size, capsuled membrane, and cell/tissue-specific homing, thereby functioning as providers of biologically active molecules and efficient vehicles to deliver these molecules to appropriate targets (25,26). In this study, the use of ADSC-derived exosomes in obesity treatment is more than a compensation for physiological functions of ADSCs in supporting WAT homeostasis; more importantly, it is a simple, efficient, cell-free therapy that can avoid the risk of neoplasia caused by ADSC supplement. Because obesity or diabetes could decrease ADSCs or impair their capacity for anti-inflammation and wound healing (21,49,50), the production and bioactivities of exosomes from these ADSCs would be influenced, thus increasing the risk for immune or metabolic disorders. Therefore, it is necessary to use ADSCs from healthy individuals for exosome isolation. Furthermore, there are still some unanswered questions that may limit the use of ADSC-derived exosomes in clinical translation. Firstly, the dosage of exosomes used in this study is possibly outside the physiological range that may elicit undesirable effects. Secondly, various cargos carried by exosomes may target different cells or tissues, producing either physiological or pathological effects. Thus, the potential toxicity of exosomes should be further evaluated. The route and frequency of exosome administration also need to be considered. Collectively, our findings propose an important exosome-mediated cross talk between ADSCs and macrophages that facilitates the immune and metabolic homeostasis in WAT, shedding light on the potential of exosome-based therapeutic approach for treating obesity and diabetes.

Acknowledgments. The authors thank Dr. Peihong Fan (Shandong University, Shandong, China) for technical assistance on ultracentrifugation, Peter Murray (St. Jude Children's Research Hospital, Memphis, TN) for providing plasmids, and Chunxing Zheng (Institute of Health Sciences, Shanghai Institutes for Biological Sciences, Chinese Academy of Sciences, Shanghai, China) for critical review and editing of the manuscript. Microscopy imaging was performed at the Microscopy Characterization Facility (Shandong University), imaging flow cytometry at State Key Laboratory of Microbial Technology (Shandong University), and transmission electron microscopy at Shandong Institute of Otolaryngology and Shandong Normal University (Shandong, China).

Funding. This study is supported by National Natural Science Foundation of China grants 81770838, 81471065, and 81270923 (to Q.W.) and Shandong Major Research Program grant 2016GSF201005 (to Q.W.).

Duality of Interest. No potential conflicts of interest relevant to this article were reported.

Author Contributions. H. Zhao and Q.S. designed the experiments, researched the data, and wrote the manuscript. Z.P., Y.B., Z.L., H.Zhan., Q.Z., and C.G. performed the experiments and provided materials. L.Z. contributed to data analysis and interpretation. Q.W. conceived the study, designed the experiments, and wrote the manuscript. Q.W. is the guarantor of this work and, as such, had full access to all of the data in the study and takes responsibility for the integrity of the data and the accuracy of the data analysis.

References

1. Hossain P, Kawar B, El Nahas M. Obesity and diabetes in the developing world–a growing challenge. N Engl J Med 2007;356:213–215

2. Hotamisligil GS. Inflammation and metabolic disorders. Nature 2006;444:860–867

3. Xu H, Barnes GT, Yang Q, et al. Chronic inflammation in fat plays a crucial role in the development of obesity-related insulin resistance. J Clin Invest 2003;112:1821–1830

4. Weisberg SP, McCann D, Desai M, Rosenbaum M, Leibel RL, Ferrante AW Jr. Obesity is associated with macrophage accumulation in adipose tissue. J Clin Invest 2003;112:1796–1808

5. Wu H, Ghosh S, Perrard XD, et al. T-cell accumulation and regulated on activation, normal T cell expressed and secreted upregulation in adipose tissue in obesity. Circulation 2007;115:1029–1038

6. Lumeng CN, Bodzin JL, Saltiel AR. Obesity induces a phenotypic switch in adipose tissue macrophage polarization. J Clin Invest 2007;117:175–184

7. Chawla A, Nguyen KD, Goh YP. Macrophage-mediated inflammation in metabolic disease. Nat Rev Immunol 2011;11:738–749

8. Wu D, Molofsky AB, Liang HE, et al. Eosinophils sustain adipose alternatively activated macrophages associated with glucose homeostasis. Science 2011;332:243–247

9. Fujisaka S, Usui I, Bukhari A, et al. Regulatory mechanisms for adipose tissue M1 and M2 macrophages in diet-induced obese mice. Diabetes 2009;58:2574–2582

10. Chinetti-Gbaguidi G, Staels B. Macrophage polarization in metabolic disorders: functions and regulation. Curr Opin Lipidol 2011;22:365–372

11. Wu J, Boström P, Sparks LM, et al. Beige adipocytes are a distinct type of thermogenic fat cell in mouse and human. Cell 2012;150:366–376

12. Shabalina IG, Petrovic N, de Jong JM, Kalinovich AV, Cannon B, Nedergaard J. UCP1 in brite/beige adipose tissue mitochondria is functionally thermogenic. Cell Reports 2013;5:1196–1203

13. Cohen P, Spiegelman BM. Brown and beige fat: molecular parts of a thermogenic machine. Diabetes 2015;64:2346–2351
14. Nguyen KD, Qiu Y, Cui X, et al. Alternatively activated macrophages produce catecholamines to sustain adaptive thermogenesis. Nature 2011;480:104–108
15. Qiu Y, Nguyen KD, Odegaard JI, et al. Eosinophils and type 2 cytokine signaling in macrophages orchestrate development of functional beige fat. Cell 2014;157: 1292–1308
16. Bassi EJ, Moraes-Vieira PM, Moreira-Sá CS, et al. Immune regulatory properties of allogeneic adipose-derived mesenchymal stem cells in the treatment of experimental autoimmune diabetes. Diabetes 2012;61:2534–2545
17. González MA, Gonzalez-Rey E, Rico L, Büscher D, Delgado M. Adipose-derived mesenchymal stem cells alleviate experimental colitis by inhibiting inflammatory and autoimmune responses. Gastroenterology 2009;136:978–989
18. González MA, Gonzalez-Rey E, Rico L, Büscher D, Delgado M. Treatment of experimental arthritis by inducing immune tolerance with human adipose-derived mesenchymal stem cells. Arthritis Rheum 2009;60:1006–1019
19. Grayson WL, Bunnell BA, Martin E, Frazier T, Hung BP, Gimble JM. Stromal cells and stem cells in clinical bone regeneration. Nat Rev Endocrinol 2015;11:140–150
20. Mizuno H, Tobita M, Uysal AC. Concise review: Adipose-derived stem cells as a novel tool for future regenerative medicine. Stem Cells 2012;30:804–810
21. Shang Q, Bai Y, Wang G, et al. Delivery of adipose-derived stem cells attenuates adipose tissue inflammation and insulin resistance in obese mice through remodeling macrophage phenotypes. Stem Cells Dev 2015;24:2052–2064
22. Tan A, Rajadas J, Seifalian AM. Exosomes as nano-theranostic delivery platforms for gene therapy. Adv Drug Deliv Rev 2013;65:357–367
23. EL Andaloussi S, Mäger I, Breakefield XO, Wood MJ. Extracellular vesicles: biology and emerging therapeutic opportunities. Nat Rev Drug Discov 2013;12:347–357
24. Colombo M, Raposo G, Théry C. Biogenesis, secretion, and intercellular interactions of exosomes and other extracellular vesicles. Annu Rev Cell Dev Biol 2014; 30:255–289
25. Lai RC, Yeo RW, Lim SK. Mesenchymal stem cell exosomes. Semin Cell Dev Biol 2015;40:82–88
26. Yeo RWY, Lai RC, Zhang B, et al. Mesenchymal stem cell: an efficient mass producer of exosomes for drug delivery. Adv Drug Deliv Rev 2013;65:336–341
27. Lai RC, Arslan F, Lee MM, et al. Exosome secreted by MSC reduces myocardial ischemia/reperfusion injury. Stem Cell Res (Amst) 2010;4:214–222
28. Lin KC, Yip HK, Shao PL, et al. Combination of adipose-derived mesenchymal stem cells (ADMSC) and ADMSC-derived exosomes for protecting kidney from acute ischemia-reperfusion injury. Int J Cardiol 2016;216:173–185
29. Hannafon BN, Trigoso YD, Calloway CL, et al. Plasma exosome microRNAs are indicative of breast cancer. Breast Cancer Res 2016;18:90
30. Ventura S, Aryee DN, Felicetti F, et al. CD99 regulates neural differentiation of Ewing sarcoma cells through miR-34a-Notch-mediated control of NF-κB signaling. Oncogene 2016;35:3944–3954
31. Zhang B, Yin Y, Lai RC, Tan SS, Choo AB, Lim SK. Mesenchymal stem cells secrete immunologically active exosomes. Stem Cells Dev 2014;23:1233–1244
32. Deng ZB, Poliakov A, Hardy RW, et al. Adipose tissue exosome-like vesicles mediate activation of macrophage-induced insulin resistance. Diabetes 2009;58: 2498–2505
33. Singh PP, Smith VL, Karakousis PC, Schorey JS. Exosomes isolated from mycobacteria-infected mice or cultured macrophages can recruit and activate immune cells in vitro and in vivo. J Immunol 2012;189:777–785
34. Rahman MJ, Regn D, Bashratyan R, Dai YD. Exosomes released by islet-derived mesenchymal stem cells trigger autoimmune responses in NOD mice. Diabetes 2014;63:1008–1020
35. Boelens MC, Wu TJ, Nabet BY, et al. Exosome transfer from stromal to breast cancer cells regulates therapy resistance pathways. Cell 2014;159:499–513
36. Vasquez-Dunddel D, Pan F, Zeng Q, et al. STAT3 regulates arginase-I in myeloid-derived suppressor cells from cancer patients. J Clin Invest 2013;123: 1580–1589
37. Monticelli LA, Buck MD, Flamar AL, et al. Arginase 1 is an innate lymphoid-cell-intrinsic metabolic checkpoint controlling type 2 inflammation. Nat Immunol 2016; 17:656–665
38. Pegg AE. Functions of polyamines in mammals. J Biol Chem 2016;291:14904–14912
39. Carrière A, Jeanson Y, Berger-Müller S, et al. Browning of white adipose cells by intermediate metabolites: an adaptive mechanism to alleviate redox pressure. Diabetes 2014;63:3253–3265
40. Kusminski CM, Bickel PE, Scherer PE. Targeting adipose tissue in the treatment of obesity-associated diabetes. Nat Rev Drug Discov 2016;15:639–660
41. Scherer PE. Adipose tissue: from lipid storage compartment to endocrine organ. Diabetes 2006;55:1537–1545
42. Sun K, Kusminski CM, Scherer PE. Adipose tissue remodeling and obesity. J Clin Invest 2011;121:2094–2101
43. Munder M, Eichmann K, Modolell M. Alternative metabolic states in murine macrophages reflected by the nitric oxide synthase/arginase balance: competitive regulation by CD4+ T cells correlates with Th1/Th2 phenotype. J Immunol 1998;160: 5347–5354
44. Szanto A, Balint BL, Nagy ZS, et al. STAT6 transcription factor is a facilitator of the nuclear receptor PPARγ-regulated gene expression in macrophages and dendritic cells. Immunity 2010;33:699–712
45. Lai RC, Yeo RW, Tan KH, Lim SK. Mesenchymal stem cell exosome ameliorates reperfusion injury through proteomic complementation. Regen Med 2013;8: 197–209
46. Robbins PD, Dorronsoro A, Booker CN. Regulation of chronic inflammatory and immune processes by extracellular vesicles. J Clin Invest 2016;126:1173–1180
47. Liu GY, Liu J, Wang YL, et al. Adipose-derived mesenchymal stem cells ameliorate lipid metabolic disturbance in mice. Stem Cells Transl Med 2016;5:1162–1170
48. Phinney DG, Pittenger MF. Concise review: MSC-derived exosomes for cell-free therapy. Stem Cells 2017;35:851–858
49. Cianfarani F, Toietta G, Di Rocco G, Cesareo E, Zambruno G, Odorisio T. Diabetes impairs adipose tissue-derived stem cell function and efficiency in promoting wound healing. Wound Repair Regen 2013;21:545–553
50. Strong AL, Bowles AC, Wise RM, et al. Human adipose stromal/stem cells from obese donors show reduced efficacy in halting disease progression in the experimental autoimmune encephalomyelitis model of multiple sclerosis. Stem Cells 2016; 34:614–626